Pore pressure estimation by using a modified boundary element method

Wildney W. S. Vieira, Egor Sibiryakov*, Boris Sibiryakov* and Lourenildo W. B. Leite, UFPA, Brazil, RAS-NSU*, Russia*

Abstract

This paper resumes a research for solving numerically a three-dimensional problem of elastic stationary oscillations, with a particular application to the case pore pressure in sedimentary rocks. The method can be used not only for applications in oil and gas exploration, but also for modeling buried structures and structural components such as foundations, tunnels, trenches, cavities, etc. The basis of this method is the construction of integral equations kernels as a response to an analogue Delta loading, or to its derivatives. The finiteness of the kernels gives the possibility to increase accuracy in many orders, and to solve the elastic problem in the case of discontinuity in the normal vector to the contouring S surface to the goal volume V. As an example, we show that the variation of the characteristics of the static stress state under the influence of pore pressure depends essentially on the contact geometry, and a little on the type of boundary condition at the contact.

Introduction

This paper concerns the application of the theory of the linear elastic mixed boundary value problem (MBVP) of solids aiming at geological basin modeling with applications to oil and gas exploration, as decribed by Sibiriakov et al. (2016). We look, among other goals, for mapping low and high pressure zones that serve as natural suction pumps, where a reservoir is necessarily related to a low pressure zone in the subsurface, besides the necessary geological conditions. We also deal several aspects of the theory for a typical reservoir model as a numerical experiment about effective pore pressure, and the specific application in this paper is the problem of the effective pressure (p_{eff}) and anomalous high porous pressure (p_{por}).

The problem is to calculate the stress-strain distribution in solids, modeling a sedimentary basin, using maps of $v_P(\mathbf{x})$ and $v_S(\mathbf{x})$ velocities, and density $\rho(\mathbf{x})$.

The real data can be obtained from special surveys with 3D sensor components, where a large amount of P wave information is conventional. The S wave velocity information can also be obtained from VSP technology, and by petrophysical measurements (Biondi, 2010; Galperin, 1985).

To solve the elastic problem is necessary to know the boundary geometries, and the distribution of the elastic parameters in the subsurface. The present model considers only isotropic layers, and the model is discretized in an uniform 3D grid, where the layer cells forming the geological structure have constant elastic parameters.

Methodology

The construction of the physical problem starts with the elastodynamic wave propagation equation in the Cartesian system with $(i = 1,2,3; x,y,z)$, where $\mathbf{u}(t,\mathbf{x})$ is the displacement vector with components $u_i(t,\mathbf{x})$, considering the case of oscillatory temporal condition $u_i = U_i e^{i\omega t}$:

$$\Delta U_i + k^2 U_i + \frac{\lambda+\mu}{\mu}\text{Grad}_i\text{Div}\mathbf{U} = 0, \quad (k^2 = \frac{\rho}{\mu}\omega^2), \qquad (1)$$

where ΔU_i is the Laplace operator on the displacement u_i and U_i; λ and μ are the Lamé linear elastic strain-stress moduli; ρ is the body volume density; and ω the angular frequency of stationary oscillations.

The loading vector components, $p_i = \sigma_{in_0}$ (traction or compression), are the pressure (force per unit area) components expressed by the formula

$$p_i = \sum_{k=1}^{k=3} \sigma_{ik} n_k = \sigma_{in_0}, \qquad (2)$$

where σ_{ik} is the stress tensor, n_k is the projection cosine along the unit normal vector $\mathbf{n}$ to the S surface, and σ_{in_0} can be calculated by Hooke's law, and also by the rule of tensor projections; therefore, the loading is not defined by the simple normal stress. A complementary expression for σ_{ik} is given by

$$\sigma_{ik} = \lambda\text{Div}\mathbf{U}\delta_{ik} + \mu(\frac{\partial U_i}{\partial x_k} + \frac{\partial U_k}{\partial x_i}), \qquad (3)$$

$$\text{Div}\mathbf{U} = \theta = \frac{\partial U_i}{\partial x_i} + \frac{\partial U_j}{\partial x_j} + \frac{\partial U_k}{\partial x_k}. \qquad (4)$$

In practical terms, if we have a reservoir at depth z_0 (say, 2000m) we can calculate the loading $p_i = \sigma_{ik} n_k$ if we have the displacement vector to calculate the strain tensor, and by Hooke's law calculate the loading p_i. We can also use the effect of the gravity weight to calculate the loading, because in this case, we are solving for the nonhomogeneous equation of equilibrium given by

$$\mu\Delta U_i + (\lambda+\mu)\text{Grad}_i\text{Div}\mathbf{U} = -\rho g \delta_{iz}, \qquad (5)$$

under the condition that $p_i = 0$ at the surface ($z = 0$). But, the atmospheric pressure can be assigned to the normal component, and zeros to the tangential components.

The solution for equation (1) is found in the form of a convolution with a kernel that satisfies the equation at any

fixed point $\mathbf{x_0}$ of a closed volume V, that can be arbitrarily close to the enclosing S surface. The integration is carried out over the position variable $\mathbf{x}$, and calculated with a surface element $dS_{\mathbf{x}}$; i.e.,

$$U_i(\mathbf{x_0}) = \int_S M_{ik}(\mathbf{x_0},\mathbf{x}) F_k(\mathbf{x}) dS_{\mathbf{x}}, \tag{6}$$

where $M_{ik}(\mathbf{x_0},\mathbf{x})$ is the Green's tensor (also called Green's dyadic) function, $\mathbf{F}$ corresponds to the called the potential vector, or fitting boundary vector, and the displacement vector $\mathbf{U}$ is calculated such that the displacement satisfies equation (1), and the boundary conditions (Eskola, 1992).

One classical description for the tensor M_{ik} in formula (6) is given by Kupradze (1963) for a 3D full-space (free-space), as the tensor of the fundamental solution for equation (1) given by

$$M_{ik}(\mathbf{x_0},\mathbf{x}) = \frac{1}{\mu}\left(\frac{\cos(kr)}{r}\delta_{ik} + \frac{1}{k^2}\frac{\partial^2}{\partial x_i \partial x_j}\left[\frac{\cos(kr)}{r} - \frac{\cos(\gamma kr)}{r}\right]\right), \tag{7}$$

where δ_{ik} is the Kronecker delta, and

$$r = \sqrt{(x_0 - x) + (y_0 - y) + (z_0 - z)} \tag{8}$$

is the distance between the fixed, $\mathbf{x_0}$, and integration, $\mathbf{x}$, points; $\gamma = \frac{v_S}{v_P} = \sqrt{\frac{\mu}{\lambda+2\mu}}$ velocity ratio, and x_i are the projections of the vector $\mathbf{r}$ directed from the fixed point $\mathbf{x_0}$ to the integration point $\mathbf{x}$ for the Cartesian coordinate system (x,y,z). For the static case, i. e., for $kr \ll 1$, the full-space tensor (7) is simplified to the a fundamental solution with the form

$$M_{ik}(\mathbf{x_0},\mathbf{x}) = \frac{1}{2\mu(\lambda+2\mu)}\left[(\lambda+\mu)\frac{\partial r}{\partial x_i}\frac{\partial r}{\partial x_k} + (\lambda+3\mu)\delta_{ik}\right]\frac{1}{r(\mathbf{x_0},\mathbf{x})}, \tag{9}$$

that has several disadvantages due to non-integrable singularities, except for the term with the Kronecker δ_{ik} function.

The loading $P_{ik}(\mathbf{x_0},\mathbf{x})$ is obtained with respect to the stress tensor M_{ik} of formula (9), and it is given by

$$\begin{aligned}\mathbf{P_0^x}\{M_{ik}\}(\mathbf{x_0},\mathbf{x}) = \quad & 2\mu\frac{\partial \Gamma_{ik}}{\partial \mathbf{n_0}} + \lambda \mathbf{n_0}\mathrm{Div}_{\mathbf{x_0}}(\Gamma_{ik}) \\ & + \mu[\mathbf{n_0}, \mathrm{Rot}_{\mathbf{x_0}}\Gamma_{ik}],\end{aligned} \tag{10}$$

where the essence being to calculate the loading vector at the fixed point $\mathbf{x_0}$, the first term is the directional derivative $(\frac{\partial}{\partial \mathbf{n_0}})$, the middle term includes the divergence of Γ_{ik}, and the last term is the cross product between $\mathbf{n_0}$ and $\mathrm{Rot}_{\mathbf{x_0}}(\Gamma_{ik})$, that results in

$$\begin{aligned}P_{ik}(\mathbf{x_0},\mathbf{x}) = \quad & \frac{1}{\lambda+2\mu}\left\{\left[\mu\delta_{ik} + 3(\lambda+\mu)\frac{\partial r}{\partial x_i}\frac{\partial r}{\partial x_k}\right]\frac{\partial}{\partial \mathbf{n_0}}\frac{1}{r}\right. \\ & \left. + \mu\left[\cos(\mathbf{n_0},x_k)\frac{\partial}{\partial x_i}\frac{1}{r} - \cos(\mathbf{n_0},x_i)\frac{\partial}{\partial x_k}\frac{1}{r}\right]\right\},\end{aligned} \tag{11}$$

where $\mathbf{n_0}$ is the unit normal vector at a fixed point $\mathbf{x_0}$ on the S surface.

The loading tensor (11) gives the possibility to find a solution for the MBVP of the second kind, where the loading vector p_i is known on the boundary, what is necessary to find the displacement vector in the volume V. In this case the problem is reduced to finding a solution for the system of the 2D integral equations that are not regular, but singular integral equations; i.e., the kernels are not integrable, and the integrals should be calculated in the Principle Value (P.V.) sense, and the last term in the loading tensor (11) causes this mentioned singularity. In practice, the use of such type of kernels are the cause for loosing accuracy.

Now we discuss the shortcomings of the fundamental solutions. If the loading vector p_i is known on the S surface, it is possible to calculate the correspondent potential vector, F_k, $(k = 1,2,3)$, by solving the system of integral equations of the Fredholm type of the second kind given in the form

$$p_i(\mathbf{x_0}) = F_i(\mathbf{x_0}) - \frac{1}{2\pi}\int_S P_{ik}(\mathbf{x_0},\mathbf{x}) F_k(\mathbf{x}) dS_{\mathbf{x}}, \tag{12}$$

then as a result it becomes easier to calculate the displacement vector $\mathbf{U}$ by using the integral (6). The quantity p_i is given by formula (2), and P_{ik} by formula (11).

The displacement means the amplitude responses for the half-space, under the condition that the surface normal δ-loading, $p_n = \delta(S)$, is given by

$$\delta(S) = -\frac{1}{2\pi}\int_0^\infty k_r J_0(k_r r_\tau) dk_r, \tag{13}$$

where k_r is the mnemonic integration variable (k is the effective spatial frequency corresponding to the S waves). Also, all the dimensions of the involved quantities, $\delta(S)$, p_i, M_{ik}, P_{ik}, Γ_{ik}, are compensated by the dimension of the potential vector $\mathbf{F}$.

The finite analogue of Delta function can be written as

$$\delta_1(S) = -\frac{1}{2\pi}\int_{k_r=0}^{k_r=N} k_r J_0\left(r_\tau\sqrt{k_r^2 + 2k^2}\right) dk_r. \tag{14}$$

The limits of integration is now from 0 to the inverse of the sampling interval, i. e., $N \sim h^{-1}$. Formally, the finiteness of the kernel causes the necessity to solve the Fredholm equation of the first kind (loosing conditioning) for finding the potential vector, and also loosing completeness.

On the contact skeleton-fluid the normal component of the loading vector is equal to the fluid pressure, and the tangential components of the loading vector are equal to zero ($p_n = p_0$, $p_{\tau 1} = p_{\tau 2} = 0$). On the interface between two solid bodies, there are two main types of boundary conditions, rigid and slip.

The rigid contact means that there are no net forces on the interface and, despite of the interface existence, the displacement vector is continuous, and the vector summation of the loading vector is null. Taking into account that the external normal vector changes sign, and the tangential vectors coincide on the upper and lower layers, it means that:

1. $U_n^+ = -U_n^-$, $U_{\tau 1}^+ = U_{\tau 1}^-$, $U_{\tau 2}^+ = U_{\tau 2}^-$,
2. $p_n^+ = p_n^-$, $p_{\tau 1}^+ = -p_{\tau 1}^-$, $p_{\tau 2}^+ = -p_{\tau 2}^-$.

The symbols "+" and "-" stand for the upper and lower layers with respect to the S surface.

The slip contact (that can have a modification to include a friction coefficient) means that the tangential forces are zero, and only the normal component of the displacement vector is continuous, that is:

1. $U_n^+ = -U_n^-$,
2. $p_n^+ = p_n^-, \quad p_{\tau 1}^+ = -p_{\tau 1}^- = 0, \quad p_{\tau 2}^+ = -p_{\tau 2}^- = 0.$

It should be clear enough that the mixed type of boundary conditions (with rigid and slip conditions) are the most important ones for geophysics.

The Static MBVP

The new displacement tensor components give results for the static case ($k \to 0$) for the half-space in the form:

$$M_{nn} = \int_0^N J_0(k_r r_\tau) \frac{\exp(-|x_1|k_r)}{4\pi\mu(1-\gamma^2)} \left(1 + k_r|x_1|(1-\gamma^2)\right) dk_r, \quad (15)$$

$$M_{nr} = \int_0^N -J_0'(k_r r_\tau) \frac{\exp(-|x_1|k_r)}{4\pi\mu(1-\gamma^2)} \left(-\gamma^2 + k_r|x_1|(1-\gamma^2)\right) dk_r, \quad (16)$$

$$M_{rn} = \int_0^N -J_0'(k_r r_\tau) \frac{\exp(-|x_1|k_r)}{4\pi\mu(1-\gamma^2)} \left(\gamma^2 + k_r|x_1|(1-\gamma^2)\right) dk_r, \quad (17)$$

$$M_{rr} = \int_0^N \left[2J_0(k_r r_\tau)(1-\gamma^2) + J_0''(k_r r_\tau)(1-2\gamma^2) + k_r|x_1|(1-\gamma^2)J_0''(k_r r_\tau)\right] \frac{\exp(-|x_1|k_r)}{4\pi\mu(1-\gamma^2)} dk_r, \quad (18)$$

$$M_{\varphi\varphi} = \int_0^N \left[J_0(k_r r_\tau) - J_0''(k_r r_\tau)(1-2\gamma^2) - k_r|x_1|(1-\gamma^2)(J_0(k_r r_\tau) + J_0''(k_r r_\tau))\right] \frac{\exp(-|x_1|k_r)}{4\pi\mu(1-\gamma^2)} dk_r. \quad (19)$$

Solving the MBVP, the boundary conditions should be satisfied. In the first step (and in the main ones) of computing the potential vector, the fixed point, $\mathbf{x_0}$, is on the surface (on the volume boundary). If the potential vector, F_k, is already known, for computing the other parameters (strains or stress), then the fixed point is inside the volume V. It may be difficult to digest that inside the volume V of a homogeneous medium there are no normal and tangential vector components, and in this case (i. e., for the calculation of displacements or strains inside the volume) these components have the meaning of a virtual (not real) surface inside the volume.

Effective Pressure, Rigid and Slip Contacts

Often, the effective properties, p_{eff}, of porous granular media does not depend on the confining (external) pressure, p_{conf}, but on the difference between confining and porous, $p_0 = p_{\text{por}}$, (fluid) pressures, as $p_{\text{eff}} = p_{\text{conf}} - p_0$.

The opinion that porous pressure opposes the approximation of contacts is not correct, because pressure is a scalar quantity, and only surface forces can approximate or separate contacts. Sometimes it is necessary to use a dimensionless factor of unknown nature for p_{eff}.

Now, let's consider the physics for a minimum representative volume which consists of grains with flat contacts (called here platforms) as shown in figure 1. The problem is that porous pressure (p_0) in granular media can cause two opposite processes. As a first case, it is to increase the distances between grain centers, and this effect is significant around the edges (indicated in the right side of figure 1). As a second case, it is to decrease the distance between grain centers (indicated in the left side of figure 1). The question that we raise here is, which effect is stronger and prevails?

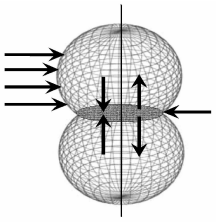

Figure 1: Geometry of grains with a contact surface, called platform by being flat, and the force distribution around the surface shown by arrows.

In the literal sense, granular media is not continuous. Of course, this means that we can have some average effective properties, but it is impossible to understand the dependence of the effective properties on external parameters in the framework of continuous medium by using "average" forces in every point.

In order to analyze the dependence of the effective pressure (p_{eff}) on porous pressure (p_0), and on the structure of the porous state, it is necessary to solve the static elastic problem of the mixed boundary type. The boundary conditions described for the part of the grain (spherical) that is in contact with fluid is obvious; i.e., the normal component of the loading vector is equal to the porous pressure, and the tangential components are zero.

As for the boundary conditions for contact platforms, between grains, there are two variants: (1st) the rigid contact (platforms are welded), where the displacement vector is null; (2nd) slip contact, where the normal component of the displacement vector and tangential components of the loading vector are null. So, the effective pressure (p_{eff}) is composed by the confining pressure, and by the average normal loading vector on the contact platforms.

Numerical Example

Now, it is interesting to solve this problem for a grain with 6 contact surfaces, as described below. This experiment gives an opportunity to test not only the new tensor displacement formulas (15-19), but also to understand the dependence of the effective properties of granular media on the contact area (platforms), and on the type of the boundary conditions.

The S surface corresponds to a sphere of unit radius with six contact platforms, as shown in figure 2. The size of the platform is determined by the parameter h_0, that is the distance from the sphere center to the center of the contact platform. The surface parametric equation for the x-coordinate is, for example, given by

$$\begin{cases} \text{if } \sin\theta\cos\varphi > h_0, & \text{then } x = h_0, \\ \text{else if } \sin\theta\cos\varphi < -h_0, & \text{then } x = -h_0, \\ \text{else } x = \sin\theta\cos\varphi. \end{cases} \quad (20)$$

Similar relations hold for the y and z coordinates. Such surface assigning is more convenient than assigning 7 surfaces (6 flat platforms and 1 that corresponds to the remaining of the sphere in contact with the fluid). The platform contours are not circumferences, instead they are close to a polygon (see figure 3). To construct the

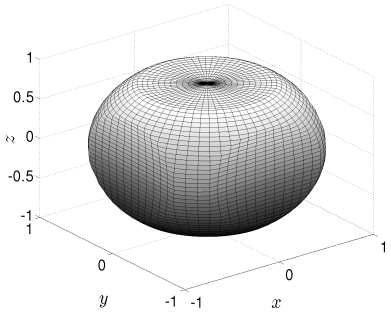

Figure 2: The clipped ball model with six flat contact areas (platforms) represented in Cartesian coordinates (x,y,z), and to be submitted to stress loading and boundary conditions.

surface is necessary to run over the parameter θ from 0 to π rd (radians as on spherical coordinates), and over the parameter φ from 0 to 2π rd.

Figure 3 is the Indicator surface presented to clarify the next figures, the role of the parameters θ and φ, and $h_0 = 0.8$. The indicator parameter is given by $I = 1$ for the platform (solid-solid contact), and by $I = 0$ for the remaining part of the sphere (solid-fluid contact).

The problem is reduced to the elastic mixed type boundary condition to calculate the average normal component of the loading vector on the platforms (solid-solid contact) for different values of h_0 (i.e., different areas of contact), and for different boundary condition (solid-solid, either rigid or slip conditions). The average normal component corresponds to a second summation to obtain the effective pressure (p_{eff}).

The Lamé parameters and the porous pressure were set equal to 1; therefore, the result is proportional to p_0. The grid was defined with 59 mesh nodes for the parameter θ, and 60 for the parameter φ (i.e., the intervals were $h_\theta = \frac{\pi}{60}$ and $h_\varphi = \frac{\pi}{30}$). The h_0 parameter had values set to: 0.8, 0.85, 0.9 and 0.95. Also, the numerically calculation was performed for the two mentioned types of conditions (rigid and slip boundaries). The size of the final matrix (for the calculation of the potential vector by matrix inversion) was 10620×10620. This matrix includes either the computation for

$$p_i(\mathbf{x}_0) = -\int_S P_{ik}(\mathbf{x}_0,\mathbf{x})F_k(\mathbf{x})dS_{\mathbf{x}},$$

or for

$$U_i(\mathbf{x}_0) = \frac{1}{2\pi}\int_S M_{ik}(\mathbf{x}_0,\mathbf{x})F_k(\mathbf{x})dS_{\mathbf{x}},$$

and the selection depends on the boundary conditions. If the potential vector $\mathbf{F}$ is known, then the loading vector given by

$$p_i(\mathbf{x}_0) = -\int_S P_{ik}(\mathbf{x}_0,\mathbf{x})F_k(\mathbf{x})dS_{\mathbf{x}},$$

can be calculated. The average of the normal component of the loading vector is calculated by integration over the contact platforms by

$$\bar{p}_n(\mathbf{x}_0) = \frac{1}{S}\int_S p_n(\theta,\varphi)I(\theta,\varphi)dS, \qquad (21)$$

where S is the total surface area.

Figure 3 stands as another representation of the clipped ball model associated with the S surface for analysis of discontinuities. In this case, it is represented in the θ and φ coordinates by the I-indicator, that means: $I = 1$ for the flat contact area, and $I = 0$ for the spherical area. The surface parameter height is $h_0 = 0.8$. The boundary conditions for both I-cases are as follows:

1. if the point is on the spherical side of figure 2, and on the area for $I = 0$ of figure 3, then the normal component of the loading vector, (p_n, equation (2), is equal to the pore pressure ($p_n = p_0$), and the tangential components are zero ($p_\tau = 0$).
2. if the point is on the flat side of figure 2, and on the area for $I = 1$ of figure 3, then the normal component of the loading vector, (p_n, equation (2), is equal zero ($p_n = 0$), and either the tangential components of the displacement vector are zero (rigid contact condition, $U_\tau = 0$), or the tangential components of the loading vector (p_τ, equation (2) are zero (for slip contact condition, $p_\tau = 0$).

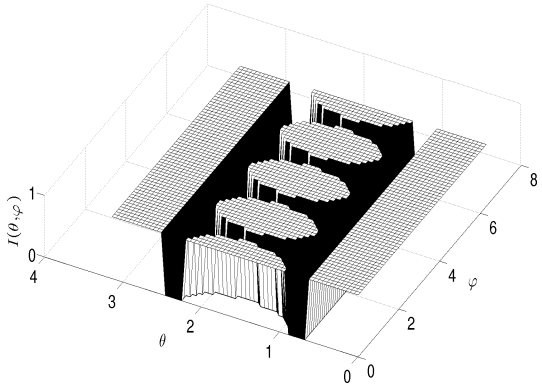

Figure 3: Discontinuity surface images of the clipped ball model with six flat areas of figure 2 in the θ and φ cylindrical coordinates using the I-indicator function, with the conditions: $h_0 = 0.8$; $I = 1$ in the flat contact area; and $I = 0$ on the boundary part with the presence of fluid. The amplitude scale shows 1 and 0, and the six polygonal shapes of the flat contact area. On the two lateral parts $I = 1$, and have an extended flat form.

The singularity of the kernels (despite of the singularity type) causes in all cases the necessity for calculating improper integrals. This means that it is necessary to add to the numerical summation an additional term based on an analytical calculation (an integral on a small area that includes a point of function singularity). But, the accuracy of such additional term is low enough (h^2); therefore, it makes no sense using high order integration formulas; that means, stay with Simpson quadrature.

The finite kernels give the possibility to answer interesting questions about the dependence of the accuracy of the elastic problem solution, and about the integration formula for accuracy estimation. The question is: Is it justifiable to use high order formulas for the integral calculation? The answer is based on the found results that showed to be very interesting and surprising.

Different integral formulas give different potential vectors, but the loading vectors (final result of the elastic problem

solution) proved to be identical, and the maximum difference was in the order of 10^{-9}. The question now is: What is the reason for this type of result? The answer is that in this case the integral is approximated by a finite summation, also the kernel satisfies the equation of equilibrium exactly, and the dependence between displacement and loading vectors are calculated analytically, i.e., it is also exact. For example, if in the formula

$$p_i(x_0) = -\frac{1}{2\pi}\int_S P_{ik}(x_0,x)F_k(x)dS_x,$$

we denote $F_k(x)dS_x$ as a new $F_k(x)$, it means that the accuracy of the $U_i(p_i)$ does not depend on the order of the integration formula (of course, if the displacement vector is calculated by the same integration formula); therefore, it means that there is no need to calculate integrals.

It is possible from the beginning to use summations, e.g., instead of integrals, use a form like

$$U_i(x_0) = \sum_S M_{ik}(x_0,x)F_k(x),$$

where the summation is over the surface integration points. The loading vector depends on the displacement vector analytically; i.e.,

$$p_i(x_0) = -\sum_S P_{ik}(x_0,x)F_k(x), \tag{22}$$

where $P_{ik}(x_0,x)$ is the loading vector under the condition that M_{ik} is the displacement tensor.

So, by changing the classical Delta function by a finite analogue for the numerical methods gives the possibility to solve the elastic problems with mixed type boundary conditions (not only the static, the dynamic also), and to use finite summation for the solution instead of integrals.

Results

Figure 4 shows only part of the huge matrix to calculate the potential vector for the clipped ball calculated by the linear system given by the formulas (15-19). The problem is of the mixed type, and this figure is a part of the matrix of the system, that contains both M_{ik} and P_{ik} and projections, where the mentioned part contains P_{ik} with the large values, and M_{ik} with the smaller values. The model parameter was set as $h_0 = 0.85$, boundary conditions of rigid contact, and the result of the matrix inversion was stable and reliable.

Figure 5 shows the normal component of the potential vector (for the same conditions as in figure 4). The small absolute values of the potential vector is caused by using the formulas

$$U_i(\mathbf{x_0}) = \sum_S M_{ik}(\mathbf{x_0},\mathbf{x})F_k(\mathbf{x}), \tag{23}$$

instead of,

$$U_i(\mathbf{x_0}) = \frac{1}{2\pi}\int_S M_{ik}(\mathbf{x_0},\mathbf{x})F_k(\mathbf{x})dS_\mathbf{x}, \tag{24}$$

that means the absence of the multiplication by the surface element $dS_\mathbf{x}$, that would be compensated by multiplying by the large values of M_{ik}.

Figure 6 shows the normal component of the loading vector, p_n, under the same conditions as given in figures 4 and 5, as a result of the convolution of the potential vector, $F_k(\mathbf{x})$, with the modified stress tensor, $P_{ik}(\mathbf{x_0},\mathbf{x})$, of the fundamental loading; i. e.,

$$p_i(\mathbf{x_0}) = -\sum_S P_{ik}(\mathbf{x_0},\mathbf{x})F_k(\mathbf{x}). \tag{25}$$

It is visible that the loading depends slightly on the parameter φ, and this means that the contacts are interacting with each other. With a further decrease in the size of contacts (i. e., by increasing the parameter h_0), the loading (on the upper and lower platforms) ceases to depend on the φ coordinate.

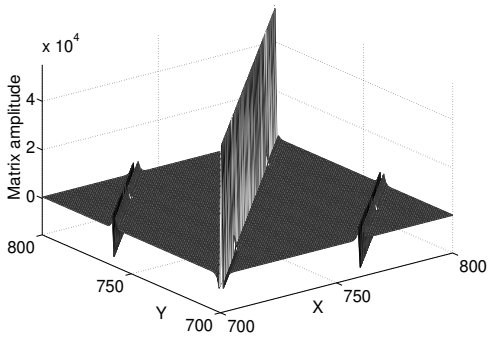

Figure 4: Fragment of the huge matrix system (15-19) that contains P_{ik} (large values) and M_{ik} (small values) for calculating the potential vector $F_n(\theta,\varphi)$, for $h_0 = 0.85$ and rigid contact.

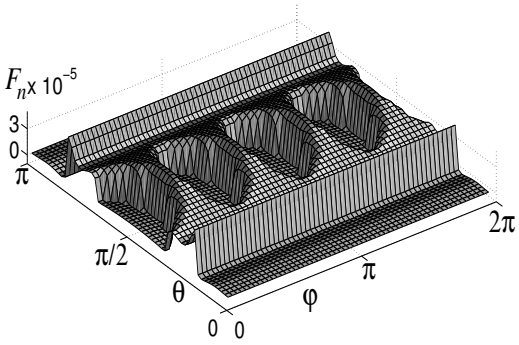

Figure 5: Dependence of the normal component of the potential vector, F_n, for reliability and stability. This result says that it is a pleasant fact that the part of the surface bordered by the fluid, where the normal loading was well defined, did not change after the numerical calculations for the potential vector F_n. The values were: $h_0 = 0.85$; and the parameters θ and φ: $0 \le \theta \le \pi$ (left axis), $0 \le \varphi \le 2\pi$ (right axis).

In all cases, the normal component of the displacement vector was defined on the contact solid-fluid (on a part of the whole surface). Also, the loading vector was computed by using a formula of the type $p_i = -\sum P_{ik}(x_0,x)F_k(x)$ (for the whole surface, including the part where the loading vector, p_i, was defined). From one point of view, the calculated loading vector on the contact fluid-solid was coincident with the prescribed conditions, and almost absolutely.

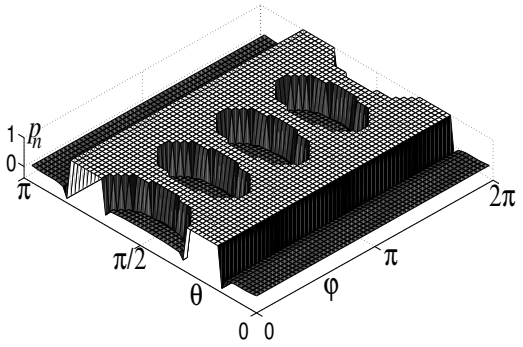

Figure 6: The normal component of the loading vector p_n for $h_0 = 0.85$, as a function of the $0 \leq \theta \leq \pi$ (left axis) and $0 \leq \varphi \leq 2\pi$ (right axis) parameters. The borders with fluid have loading p_i equal to 1. On the platform boundaries, the normal loading and maximum modulus change rapidly. This result comes from a convolution with a modified potential stress tensor given by formula (25).

Results of the dependence of the average normal component of the loading vector, $\overline{p}_n$, on the porous pressure and on the parameter h_0 (under the condition that the porous pressure is unit) is presented in Table 1.

h_0	rigid contact, $\overline{p}_n$	slip contact, $\overline{p}_n$
0.80	-0.018	-0.020
0.85	-0.031	-0.039
0.90	-0.075	-0.103
0.95	-0.342	-0.416

Table 1: Dependence of the average normal loading, $\overline{p}_n$, (as effective pressure, p_{eff}) on the h_0 parameters, and on the type of boundary contact, with the condition that the pore pressure is equal to 1. From the table, the effective pressure is proportional to the pore pressure, as can be seen from the increasing negative values on both right columns with respect to the left column.

The main difference, from the mechanical point of view, between the present method and the one by Sibiryakov and Sibiryakov (2010), is the interaction between the platforms of the grain contacts, where in the axial symmetric case, there was only two platforms, no dependence on the φ parameter, and the average normal loading was positive for the case of large enough platforms (it corresponds to reinforcement of the granular medium). But, for the present case of six platforms it is proved that the reinforcement of the granular medium to be impossible.

The common fact is that, when the area of the contact is large enough, the dependence of effective pressure (p_{eff}) on the porous pressure (p_{por}) is not significant. The smaller the grain contact area, the stronger the dependence of the effective pressure on the porous pressure, and on the type of the boundary conditions (rigid or slip). In the case of the slip contact the influence of the porous pressure on the effective pressure is larger.

The most probable areas for destruction by increasing the porous pressure are for the small contact platforms. The process of destruction will be irreversible, because the normal loading at the edge is maximum, and the beginning of rupture means decreasing of the contact area. The mechanical feedback process is that by decreasing the contact area causes the increasing of the normal component of the loading vector on the edge of the contact platform.

Conclusions

The new method applied was developed and numerically tested for the numerical solution of the linear elastic MBVPs. This method can be used to solve static and stationary oscillation problems.

The finite analogue for the dipole potential showed to be reliable and valid method to solve MBVPs.

The advantage of this method is the finiteness and the smoothness of the integral kernels, that made it possible to solve the elastic problem on surfaces, where the normal vector may have points of discontinuity.

The method showed not to depend on the accuracy of the numerical integration formula. Moreover, the method makes it possible to eliminate the use of integral equations by replacing the integrals by finite summations.

The effective pressure (p_{eff}) should have the meaning of an average normal loading, $p_{\text{eff}} = \overline{p}$, for all forms of contacts under the influence of pore pressure, instead of a subtraction ($p_{\text{eff}} = p_{\text{con}} - p_{\text{por}}$). In the present conceptual case, the effective pressure (p_{eff}) is proportional to the pore pressure (p_{por}), it has opposite sign, but the proportionality depends substantially on the contact area. If the contact area is sufficiently large, then for the rigid and for the slip contact type, the proportionality is small enough, but by reducing the contact area the proportionality becomes large enough, and the effective pressure increases.

References

Biondi, L. B., 2010, 3d Seismic Imaging: Society of Exploration Geophysicists, Tulsa, OK, USA.

Eskola, L., 1992, Geophysical Interpretation Using Integral Equations: Springer, New York, USA.

Galperin, E. I., 1985, Vertical Seismic Profiling and Its Exploration Potential: D. Reidel Publishing Company, Boston.

Kupradze, V. D., 1963, The Potential Method in Elasticity: Physics and Mathematics Issue, Moscow.

Sibiriakov, E., Sibiryakov, B., Leite, L. W. B., and Vieira, W. W. S., 2016, On a new method for the solution of the elasto-dynamic: Submitted to SEG, Geophysics.

Sibiryakov, E. P., and Sibiryakov, B. P., 2010, The structure of pore space and disjoining pressure in granular medium: Physical Mesomechanics (Special Issue), **13**, 40–43.

Acknowledgments

The authors would like to thank the sponsorship of Science Without Borders of MEC/CAPES, the Project INCT-GP, and the Project ANP-PRH-06. We extend our thanks also to the CNPQ for the scholarship.